Chinese Chemical Letters 33 (2022) 4918–4923

Contents lists available at ScienceDirect

Chinese Chemical Letters

journal homepage: www.elsevier.com/locate/cclet

Fmoc-protected amino acids as luminescent and circularly polarized luminescence materials based on charge transfer interaction

Yiran Xia, Aiyou Hao*, Pengyao Xing*

Key Laboratory of Colloid and Interface Chemistry of Ministry of Education and School of Chemistry and Chemical Engineering, Shandong University, Ji'nan 250100, China

ARTICLE INFO

Article history:
Received 26 December 2021
Revised 21 February 2022
Accepted 26 February 2022
Available online 3 March 2022

Keywords:
Fmoc-amino acids
Charge-transfer interaction
Supramolecular chirality
Multiple component coassembly

ABSTRACT

Fluorenylmethyloxycarbonyl (Fmoc)-protected amino acids are effective building blocks in self-assembled architectures at hierarchical levels, which however show limited luminescent properties and chiroptical activities. Here we introduce a charge-transfer strategy to build two-component luminescent materials with emerged circularly polarized luminescence properties. A library of Fmoc-amino acids was built, which selectively form charge-transfer complexes with the electron-deficient acceptor. Embedding in amorphous polymer matrix or physical grinding could trigger the charge-transfer luminescence with adjusted wavelengths in a general manner. X-ray diffraction results suggest the multiple binding modes between donor and acceptor. And, the solution-processed coassembly could selectively exhibit circularly polarized luminescence with high dissymmetry g-factors. This work illustrates a noncovalent charge-transfer strategy to construct luminescent and chiroptical organic composites based on the easy-accessible and economic chiral N-terminal aromatic amino acids.

Amino acids are basic units for peptides and proteins to accomplish their complicated function and structure. Peptides and oligopeptides have proven to be effective building blocks for soft assemblies including hydrogel, vesicles, emulsions and helical fibers, benefiting from their abundant hydrogen bonding sites [1–5]. Similar to the short peptides, amino acids and their derivatives also possess abundant hydrogen bonding sites to initiate the aggregation into self-assemblies with hierarchical levels [6–9]. Amino acids have strong preference to afford crystalline materials with anti-parallel supramolecular β-sheet structure [8]. Covalent modification has been developed as a promising strategy to adjust the self-assembly behaviors of amino acids. Among them, π-conjugation to amino acids at N-terminal is an effective manner [10–12]. The N-terminal aromatic amino acids are appended with strong aromatic interaction site to form π-π stacking or charge-transfer (CT) complexation [13–15]. Hydrogen bonding interaction between amide group of N-terminal amino acids play keys roles in the CT complexation with electron-deficient moieties. Through CT interaction is regarded as the orthogonal interaction to the hydrogen bonds, hydrogen bonding shall assist and stabilize the CT interaction *via* a synergistic effect [16–18]. By changing the aromatic groups and amino acids, a great variety of N-terminal amino acids were designed and synthesized. The aromatic groups ranging from naphthalene, pyrene, perylene and naphthalimide groups, giving rise to multiple structures and functions. Among the diversified structures, 9-fluorenylmethyloxycarbonyl (Fmoc) group is a protecting group of amines, which is easy to synthesis, economic and could provide efficient hydrophobicity and aromatic packing interactions [19]. Over the last decades, Fmoc-amino acids and short peptides were widely utilized in hydrogel preparation, antibacterial material and other advanced applications [20–24]. One drawback of Fmoc-amino acids is the limited absorbance and emission wavelength, which fall into the ultraviolet region. Fabricating luminescent materials based on Fmoc-amino acids and short peptides have rarely been achieved.

Chirality is a basic factor of amino acids [25]. Apart from glycine, other 19 coded amino acids own L-configuration in nature. Thus N-terminal amino acids are employed to prepare chiral materials for multiple applications. For instance, our group used a series of pyrene-conjugated amino acids to produce chiroptical materials in individual and multiple-component coassemblies [26,27]. Fmoc-amino acids under specific solvent environments could form chiral assemblies, which however exhibit poor chiroptical activities due to the fluorene group [28]. To enhance the chiroptical response of Fmoc-amino acids, Liu *et al.* used fluorescent dye Thioflavine-T to coassemble with Fmoc-glutamic acids to achieve

* Corresponding authors.
E-mail addresses: haoay@sdu.edu.cn (A. Hao), xingpengyao@sdu.edu.cn (P. Xing).

https://doi.org/10.1016/j.cclet.2022.02.077
1001-8417/

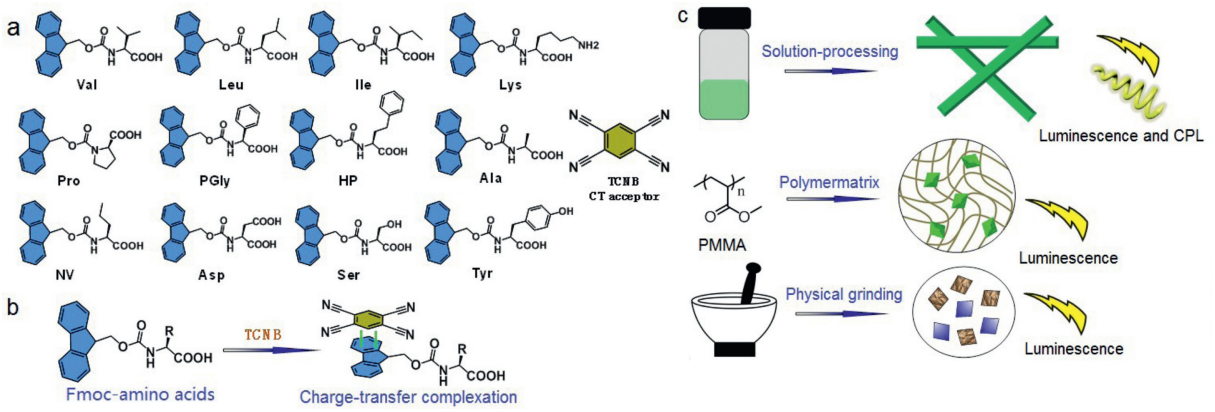

Scheme 1. (a) Molecular structures of Fmoc-amino acids and TCNB. (b) Schematic representation of charge-transfer interaction. (c) Strategies to fabricate luminescent and CPL-active materials.

active circularly polarized luminescence (CPL), which has potential in three-dimensional display and asymmetry photocatalysis applications [29]. Despite the above development, fabrication of chiroptical materials used Fmoc-amino acids has never been accomplished to the best of our knowledge.

Inspired by the CT complexation between naphthalene and electron-deficient compounds, we assumed that the fluorene group of Fmoc may behave as potential CT donor to specific acceptor such as tetracyanobenzene (TCNB), which could maintain the luminescence. Also, TCNB is capable of arousing significant bathochromic shift of luminescence due to the shortened energy gap between frontier orbitals. With the above considerations in mind, in the present work, we introduced a Fmoc-amino acid library containing different kinds of amino acid residues as donor to bind with TCNB, trying to tune the luminescent properties of Fmoc-amino acids from ultraviolet region to visible region (Scheme 1). In solution-processed coassembly, 7 of 12 applied Fmoc-amino acids form CT complexation by exhibiting yellow emission with peak at around 550 nm. Other species failed to form CT complexation due to the self-sorting process as indicated by the powder X-ray diffraction results. Using amorphous polymer matrices or physical grinding, all Fmoc-amino acids could form CT complexation due to the compact packing between CT donor and acceptors, which is a general way to construct emissive materials in the solid state. CPL spectroscopy evidences the successful fabrication of chiroptical materials based on solution-processed CT complexation, showing high dissymmetry g-factor at 10^{-2} magnitude. This work using Fmoc-amino acids as candidates to construct two-component luminescent and CPL-active organic materials, sheds light on the non-covalent strategy in supramolecular chiral material science.

In order to trigger the coassemblies and the corresponding CT emission, three strategies were employed: Solution-processed self-assembly, imbedding in polymer matrix and physical grinding in solid phase. These three approaches could produce close compact between donor and acceptors to initiate CT complexation and emission. Solution-phase coassembly was carried out in aqueous media. Concentrated stock solutions in dimethylsulfoxide (DMSO) were pre-mixed followed by the injection of bulk water with a final concentration about 3 mmol/L. Molar ratio was fixed at 1:1 based on the previous studies [27]. The dispersing in water resulted in the colloidal dispersion, which was subjected to fluorescent monitoring. The complexation between TCNB and aromatic groups in water is vulnerable to the self-sorting process that TCNB would prefer crystallizing into crystals rather than coassembly with aromatics. The self-sorting process can be thermodynamic, which means that the kinetic process of coassembly occurred immediately after dispersing in water, and the self-sorting occurs along with the incubation time at ambient condition. Thus, the incubation-time dependent fluorescent emission spectra monitoring was carried out, which were shown in Figs. 1a-c. The initial spectra of Val-TCNB system show that a new peak at around 540 nm emerges (Ex at 350 nm), which is assigned as the CT emission (Figs. S1 and S2 in Supporting information). Along with incubation time, the major CT emission blue-shifted to 510 nm, accompanied with the gradual decreased intensity. This phenomenon suggests the partial disassociation of CT complexation into individual aggregates. This behavior was also found in other coassembly systems including Val, Leu, Ile, Lys, Pro, PGly and HP. Nevertheless, Fmoc-amino acids including Ala, NV, Asp, Ser-and Tyr-failed to form fluorescent CT complexes in solution phase. The selection on coassembly or self-sorting depends on the competition between individual crystallization or coassembly. The weaker interactions in the individual crystal phase were involved, the more easily self-sorting happens. Fig. 1d summaries the decaying process along incubation time, most of the applied Fmoc-amino acids show decreased fluorescent intensity above 60%, while pro-exclusively exhibits faster fluorescent declining. Compared to the solution phase self-assembly that undergoes self-sorting, CT complexation in other phases shows stable emission from CT. Dissolving Fmoc-amino acids and TCNB in the THF solution of polymethyl methacrylate (PMMA), followed by air-drying into the amorphous and transparent thin films. The PMMA polymer matrix behaves as the solid-solution phase, which could well fix the complexes and hinders the possible disassociation. Thus, we observed the steady CT emission at 517 nm (Fig. 1e). The emission wavelength is independent to the amino acid types. It suggests the pristine crystallization capability has limited effect to the CT phase in PMMA. The third strategy to fabricate the CT complexes is physical grinding. Fmoc-amino acids and TCNB was physically mixed in a mortar, which was ground to enable the complete mixing. The homogenous solid powder exhibits yellow emission under 365 nm light irradiation. Emission spectra shown in Fig. 1f display a major peak at 550 nm, which is bathochromic-shifted. The bathochromic shift may originate from the non-solvent feature that compact CT complexation occurred under grinding. Thus, we realized CT emission from three independent strategies, with diversified emission colors. It should be noted that, in the solid samples, Tyr-shows an insignificant CT emission signal. Different to other applied Fmoc-amino acids, the Tyr-containing the phenol group, which is electron-rich. Compared to other aromatic amino acids, the phenol group is a potential competitive group to fluorene, which may interfere the charge-transfer complexation. Therefore, the CT emission of Tyr-TCNB complexation is not significant compared to other building units.

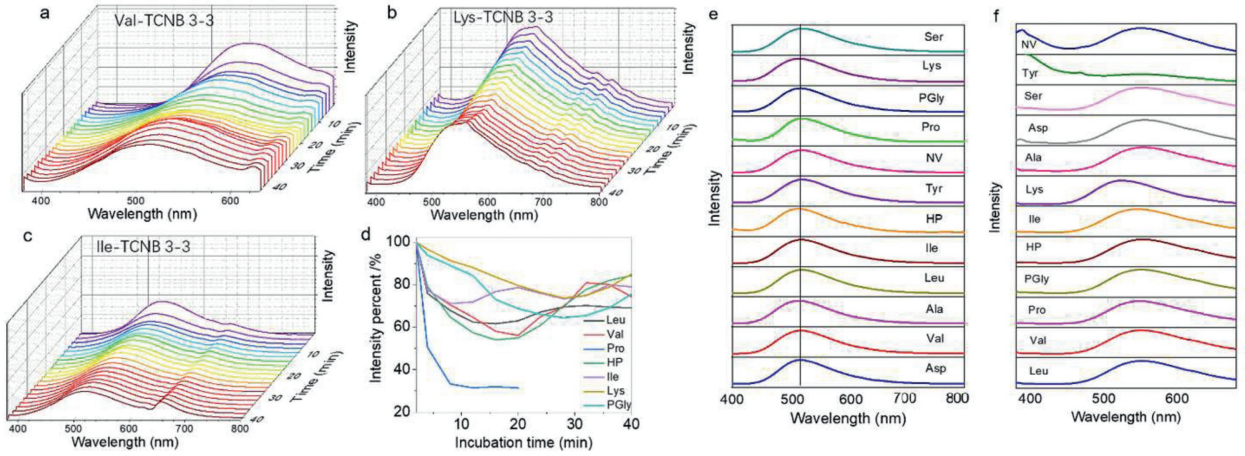

Fig. 1. Fluorescent spectra. (a-c) Incubation time-dependent fluorescent emission spectra in solution-phase self-assembly of Val-TCNB, Lys-TCNB and Ile-TCNB coassembly respectively (3 mmol/L:3 mmol/L in water). (d) Decreasing fluorescent intensity percent of different coassembly system (3 mmol/L:3 mmol/L) along with incubation time at ambient condition. (e, f) Emission spectra of coassembly in PMMA phase (3 mmol/L) and in solid-phase (by grinding).

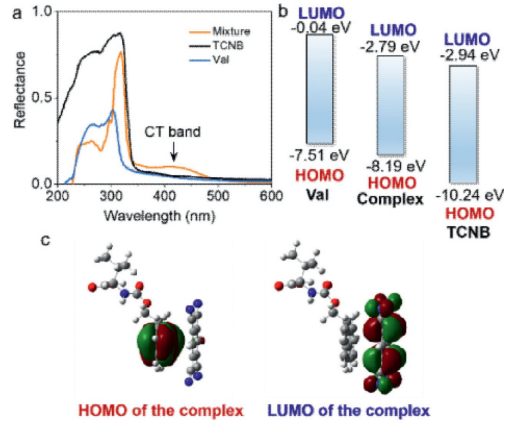

Fig. 2. (a) Diffuse reflectance spectra of Val, TCNB and their grinded mixture (1:1 by molar). (b) HOMO-LUMO energy levels of Val, TCNB and their complexes calculated based on the rcam-b3lyp/6–311 g(d) level of theory. (c) HOMO-LUMO electron cloud distribution of the CT complex.

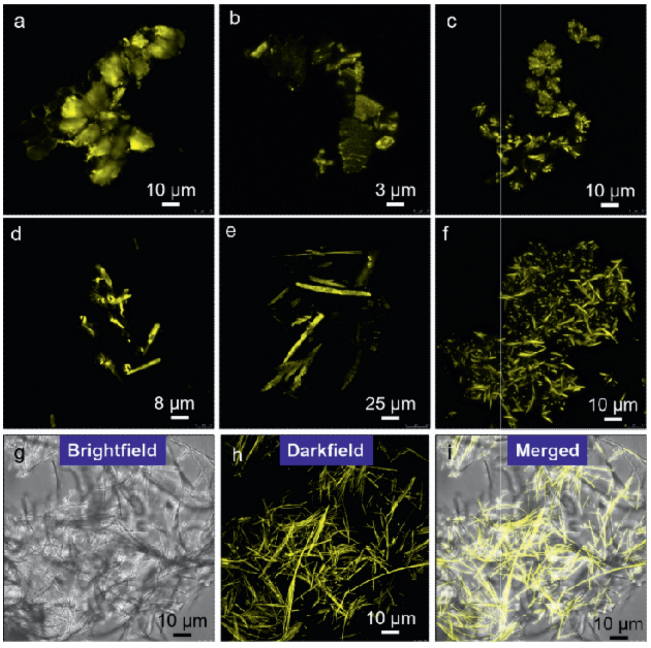

Fig. 3. (a-f) Confocal images of Val/TCNB, Leu/TCNB, Ile/TCNB, Pro/TCNB, PGly/TCNB and Lys/TCNB coassemblies in aqueous media respectively. (g-i) Confocal images of HP/TCNB coassembly under different channels. Molar ratio between Fmoc-amino acids and TCNB was fixed at 1:1 (3 mmol/L: 3 mmol/L). Ex wavelength = 420 nm.

In order to gain insights into the mechanism about CT complexation between Fmoc-amino acids and TCNB, diffuse reflectance spectra were measured. In pure solid-state, Val-and TCNB with 1:1 molar ratio was ground in a mortar. And the mixture exhibits clear yellow color. TCNB and Val-show diffuse reflectance peak at around 320 nm and 300 nm respectively, corresponding to the absorbance of cyanobenzene and fluorene group respectively. After grinding, a new band with peak centered at around 420 nm emerges. This new emerged peak is assigned to the CT band. To confirm the reflectance data, the highest occupied molecular orbital (HOMO) and the lowest unoccupied molecular orbital (LUMO) energy levels were calculated based on the energy minimalized geometries (Figs. 2b and c). The HOMO and LUMO values of Val-were determined as −7.51 and −0.04 eV respectively, while the values for TCNB are −10.24 and −2.94 eV respectively. The gap values between HOMO and LUMO for both Fmoc-amino acids and TCNB are quite large, in agreement with their absorbance at ultraviolet region. The complex with a typical geometry that TCNB and fluorene plane pack closely with a short contact distance around 3.5 angstrom. The complex gives rise to decreased HOMO-LUMO values of −8.19 and −2.79 eV. The HOMO and LUMO values of the complex are between the individual species, indicating the transfer of electron from HOMO of TCNB to LUMO of Val, which shortened the gap value, resulting in the bathochromic shift. This conclusion is further supported by the electron cloud map (Fig. 2c). Electrons distribute on fluorene at HOMO orbital while they distribute to TCNB at LUMO orbital.

Self-assemblies in aqueous media were probed by confocal laser scanning microscopy. Coassemblies in solution of various self-assemblies with CT emission were constituted by diversified morphologies under confocal (Fig. 3). Val/TCNB, Leu/TCNB and Ile/TCNB afforded plate-like morphology with lateral length up to 10 micrometers. The two-dimensional topology shows difference compared to the intrinsic fibrous assemblies from Val, Leu-and Ile-respectively. The luminescence being excited at 420 nm verifies the active participation of TCNB involving into the packing arrays of Fmoc-amino acids. And the variations of morphologies are aroused by the intercalation of TCNB to change the packing preference. In contrast, Pro/TCNB, PGly/TCNB and Lys/TCNB coassemblies exhibit fibrous structures with length and lateral width up to tens of mi-

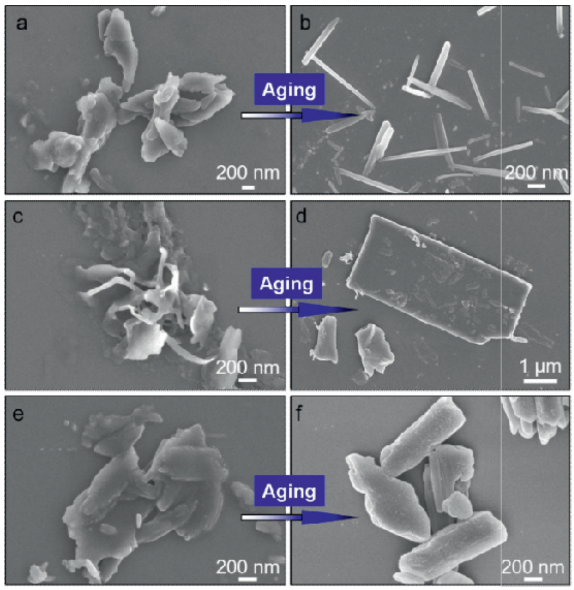

Fig. 4. SEM image tracking of self-assemblies after 2 days incubation at ambient conditions. (a, c, e) Leu/TCNB, Val/TCNB and Ile/TCNB coassembled system respectively, which were dried immediately after mixing. (b, d, f) The corresponding coassembled systems after 2 days incubation. Molar ratio between Fmoc-amino acids and TCNB was fixed at 3 mmol/L: 3 mmol/L.

crometers and several micrometers respectively (Figs. 3d-f). The rectangular shape and size indicate excellent crystallinity after the formation of complexes. The participation of TCNB does not shrink the crystallinity preference. Comparison between brightfield, darkfield and merged confocal images of HP/TCNB coassembly suggests the CT emission could be detected on the most fibers. A homogenous coassembly is thus expected. For individual HP, it self-assembled into stable hydrogel in water. However, the addition of TCNB altered the phase behavior and morphologies into microscale fibers. It is concluded that TCNB and CT interaction increases the crystallinity of Fmoc-amino acids.

From Fig. 1, it is known that along with aging period, a gradual disassociation of complexes and self-sorting occurs assisted by water. To explore the above process, scanning electron microscopy (SEM) was employed (Fig. 4, Figs. S3 and S4 in Supporting information). The mixture generated immediately was constituted by irregular particles for Leu/TCNB in water (Fig. 4a). The shape indicates the relative amorphous packing arrays. The nanoprecipitation method by dispersing DMSO stock solution into water would form microemulsion-like particles followed by the diffuse of water into DMSO oil droplets. At this stage, CT complexation and emission was allowed due to the kinetic aggregation, when no regular morphology is expected. However, the complexation in water after 2 days incubation gave rise to regularly shaped aggregates for Leu/TCNB system (Fig. 4b). The formation of well-ordered molecular arrays is controlled by thermodynamic process. It is hard to tell the phase purity based on the SEM images. The nanorods might be a mixture of self-sorted and coassembled architectures, which will be discussed in the following X-ray diffraction results. Very similar results can be found in other coassembled systems as shown in the Figs. 4c-f, where the formation of rectangular and well-shaped architectures requires incubation period. Competition between kinetic and thermodynamic process contributes to the incubation-time dependent CT emission.

To probe the molecular packing modality in coassemblies and selective self-sorting behaviors, powder X-ray diffraction (XRD) was employed (Fig. 5 and Fig. S5 in Supporting information). PGly individual aggregate show sharp XRD pattern, originating from the crystallization-induced self-assembly process (Fig. 5a). The coassemly in water possesses very similar patterns to the pristine self-assembly. However, magnified pattern suggests slight shifts. For example, peaks at 8.55, 9.44, 10.40 and 15.95 shift to 8.48, 9.29, 10.21 and 15.75° respectively. The shift values are relatively small (around ± 0.2°), which is beyond instrumental system errors. Such shifts of diffraction peaks indicate the remaining of individual assemblies with intercalated TCNB. This mode as illustrated in Fig. 5g (Packing I) is reminiscent of heterojunction structure or block copolymers. The aggregated segments inserted into the packing arrays of Fmoc-amino acids, which triggers the small shift of diffraction peaks. In comparison, HP coassembly can be assigned as the second packing mode (II, Fig. 5g). HP individually form lamellar structure due to the D-spacing ratios. However, the addition of TCNB induces the disappearance of pristine peaks with the appearance of new peaks (Fig. 5b). This pattern clearly evidences the formation of new phase without any individual assemblies of HP. In this packing modality, alternative packing of Fmoc-amino acids and TCNB is highly expected based on the previous reports and cocrystal profiles [30]. Besides, there is an example which contains both Packing I and Packing II modalities. A typical case can be found in Ile-coassembly (Fig. 5c). Coassembly owns a new emerged peak at 6.13° while other peaks are retained at their original location with slight shifts. The XRD patterns of PGly, HP and Ile-are in good consistence with the CT emission shown in Fig. 1. Other several examples can be found in Supporting information. Among the applied Fmoc-amino acids, there are five examples which could not form CT emission with TCNB. We also used XRD to analyze their binding behaviors (Figs. 5d-f and Fig. S5). In two typical cases, Ser-and Tyr (Figs. 5d and e) with additional hydroxyl group possess better solubility in water compared to other Fmoc-amino acids. The presence of TCNB would interfere the self-assembly process of Tyr-and Ser. The mixtures only show XRD patterns of TCNB without any shifts, indicating that only TCNB aggregated and Ser/Tyr-remain in a supersaturation state without aggregation. In another typical example (Fig. 5f), NV/TCNB mixture contains almost complete original XRD patterns. The final XRD pattern is an overlap of NV and TCNB individually, suggesting a self-sorting process, which is assigned as the Packing III mode (Fig. 5g). We further carried out Job's plot characterization. As shown in the Fig. S8, Val/TCNB mixture in DMSO [total concentration = 10 mmol/L] with different molar ratio displays a binding ratio of 1:2. It means that in pure solution, two TCNB molecules bind one Fmoc-group *via* a sandwich-like complexation mode. This stoichiometry is different to the solid-state probed by the X-ray structure, where an alternative packing presents.

Due to the intrinsic chirality of amino acids, the chiral Fmoc-amino acids would self-assembled into architectures with supramolecular chirality, which shall induce the emergence of chiroptical signals. The CT interaction and the corresponding luminescent properties may produce CPL activities. Circular dichroism (CD) spectra of solution-processed coassemblies exhibit a weak absorbance band ranging from 400 nm to 600 nm (Fig. 6a). Such a wide Cotton effects correspond to the emerged CT absorbance band, indicating the transfer of point chirality to CT complexes *via* CT interaction. Compared to CD spectroscopy that defines chirality at ground state, CPL represents chirality at photexcited state. After being excited, the difference between left and right-CPL could be generated as CPL active materials. Then the colloidal dispersion of coassemblies in water was subjected to CPL tests. Among the seven systems which could form CT complexation in water, only Val-and Ile-showed the CPL activities (Figs. 6b and c). Yellow CPL at around 550 nm was detected, which is assigned to the CT emission region. We successfully fabricate the chiroptical materials based on the CT of Fmoc-amino acids. Indicated by their weak CD response, it is assumed that the CPL in most cases is too weak to be de-

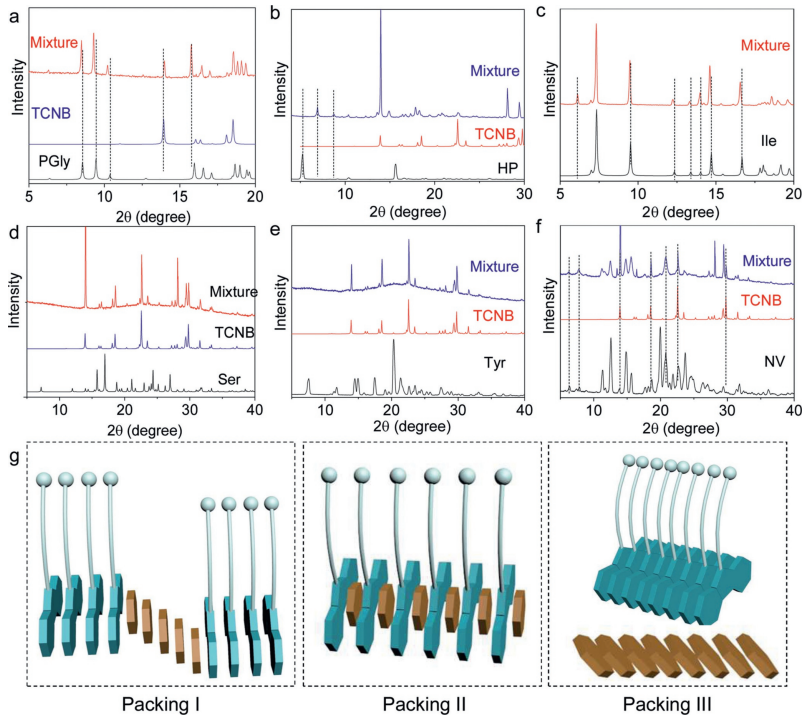

Fig. 5. (a-f) XRD comparison between different Fmoc-amino acids, TCNB and their mixtures formed in aqueous media. Concentrations of all species were fixed at 3 mmol/L. (g) Three packing modes in the coassembly mixtures. The XRD pattern of TCNB is simulated from its single crystal structure.

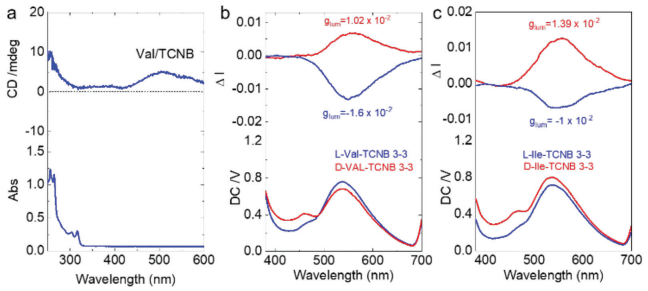

Fig. 6. (a) CD spectrum of Val/TCNB coassembly (3 mmol/L: 3 mmol/L). (b, c) CPL spectra of Val/TCNB and Ile/TCNB coassembly systems (3 mmol/L: 3 mmol/L).

tected. Nevertheless, the present two cases emit strong CPL signal with dissymmetry g-factor (glum) at 10^{-2} grade, which is among the highest values for organic species from supramolecular self-assembly. The CPL handedness is determined by the absolute chirality of amino acids, who give rise to L-CPL and R-CPL in cases of D- and L-enantiomer, respectively. Also, we explored the CPL properties in the PMMA matrices and ground samples. Unfortunately, no CPL was detected, may be due to the ill-defined molecular packing arrays.

In summary, a series of Fmoc-amino acids were chosen to construct luminescent materials with TCNB *via* CT complexation. In bottom-up solution-phase assembly, Fmoc-amino acids selectively form CT complexes with TCNB depending on the properties of amino acid residues. By using PMMA as a matrix or using physical grinding, a general CT complexation and emission was found with adjustable emission wavelength. In solution phase, a slow dissociation process was observed along with incubation periods, which contributed to the self-sorting behavior. XRD results evidence three binding modalities upon coassembly. Finally, the CT complexes in aqueous solution are CPL active. Emerged CPL signal located at around 550 nm exhibit strong dissymmetry g-factor at 10^{-2} magnitude. Based on noncovalent CT strategy, this work uses commercially available N-terminal aromatic amino acids to fabricate luminescent materials with CPL activities.

Declaration of competing interest

The authors declare no conflict of interest.

Acknowledgments

This work is supported by the Qilu Young Scholarship Funding of Shandong University. This works is also supported by the National Natural Science Foundation of China (Nos. 21901145, 22171165) and Natural Science Foundation of Jiangsu Province (No. BK20190209). We also acknowledge the financial support from Youth cross-scientific innovation group of Shandong University (No. 2020QNQT003).

Supplementary materials

Supplementary material associated with this article can be found, in the online version, at doi:10.1016/j.cclet.2022.02.077.

References

[1] G. Ghosh, R. Barman, A. Mukherjee, et al., Angew. Chem. Int. Ed. 61 (2022) e202113403.
[2] Y. Inomata, T. Sawada, M. Fujita, J. Am. Chem. Soc. 143 (2021) 16734–16739.
[3] X.Q. Dou, C.L. Feng, Adv. Mater. 29 (2017) 1604062.
[4] J. Li, J. Wang, Y. Zhao, et al., Coord. Chem. Rev. 421 (2020) 213418.
[5] T.M. Clover, C.L. O'Neill, R. Appavu, et al., J. Am. Chem. Soc. 142 (2020) 19809–19813.
[6] M. Kumar, N.L. Ing, V. Narang, et al., Nat. Chem. 10 (2018) 696–703.
[7] C. Yuan, A. Levin, W. Chen, Angew. Chem. Int. Ed. 58 (2019) 18116–18123.
[8] S. Bera, S. Mondal, S. Rencus-Lazar, et al., Acc. Chem. Res. 51 (2018) 2187–2197.
[9] Z. Zong, A. Hao, P. Xing, et al., Nanoscale 12 (2020) 20610–20620.
[10] P. Xing, Y. Li, S. Xue, et al., J. Am. Chem. Soc. 141 (2019) 9946–9954.
[11] S. Fleming, R.V. Ulijn, Chem. Soc. Rev. 43 (2014) 8150–8177.
[12] A.D. Martin, P. Thordarson, J. Mater. Chem. B 8 (2020) 863–877.
[13] Z. Wang, Y. Li, A. Hao, P. Xing, Angew. Chem. Int. Ed. 60 (2021) 3138–3147.

[14] Z. Wang, A. Hao, P. Xing, Angew. Chem. Int. Ed. 59 (2020) 11556–11565.
[15] S. An, A. Hao, P. Xing, Angew. Chem. Int. Ed. 60 (2021) 9902–9912.
[16] A. Das, M.R. Molla, B. Maity, D. Koley, S. Ghosh, Chem. Eur. J. 18 (2012) 9849–9859.
[17] A. Das, S. Ghosh, Angew. Chem. Int. Ed. 53 (2014) 2038–2054.
[18] C. Wang, D. Zhang, D. Zhu, J. Am. Chem. Soc. 127 (2005) 16372–16373.
[19] S. Fleming, S. Debnath, P.W.J.M. Frederix, Chem. Commun. 49 (2013) 10587–10589.
[20] C. Hao, Y. Gao, D. Wu, et al., Adv. Mater. (2019) 1903200.
[21] K. Tao, A. Levin, L. Adler-Abramovichab, et al., Chem. Soc. Rev. 45 (2016) 3935–3953.
[22] P. Xing, H. Chen, H. Xiang, Y. Zhao, Adv. Mater. (2018) 1705633.
[23] P. Xing, P. Li, H. Chen, A. Hao, Y. Zhao, ACS Nano 11 (2017) 4206–4216.
[24] P. Xing, S.Z.F. Phua, X. Wei, Y. Zhao, Adv. Mater. (2018) 1805175.
[25] M. Liu, L. Zhang, T. Wang, Chem. Rev. 115 (2015) 7304–7397.
[26] J. Liang, H. Zhang, A. Hao, P. Xing, ACS Appl. Mater. Interfaces 13 (2021) 29170–29178.
[27] Y. Xu, A. Hao, P. Xing, Angew. Chem. Int. Ed. 61 (2022) e202113786.
[28] R. Xing, C. Yuan, S. Li, et al., Angew. Chem. Int. Ed. 57 (2018) 1537–1542.
[29] M. Deng, L. Zhang, Y. Jiang, et al., Angew. Chem. Int. Ed. 55 (2016) 15062–15066.
[30] Z. Wang, A. Hao, P. Xing, Small 17 (2021) 2104499.